

Fatigue Behavior of Short Glass Fiber Reinforced Polyamide 66: Experimental Study and Fatigue Damage Modelling

Elouni Chebbi¹, Jamel Mars¹, Mondher Wali^{1*},
Fakhreddine Dammak¹

Received 29 January 2016; accepted after revision 05 July 2016

Abstract

The aim of the present paper is to study and model the fatigue behavior of short glass fibers reinforced polyamide-66. The effect of fiber content on the fatigue and static behavior of this composite is investigated. In such composites fatigue damage growth exhibits three stages. A continuum damage based model is presented to predict damage evolution during these three stages. Experimental results show that increasing the fiber content increases the elastic modulus and the tensile strength of the studied materials under tensile tests. However, the rupture behavior changes from ductile to brittle. Moreover increasing the fiber percentage changes the S-N curves slope and decreases the fatigue life. Analytical results predicted by the proposed model, compared to experimental ones shows good agreement and the developed model predicted fatigue damage growth in its three stages of evolution with good performance.

Keywords

fatigue damage, glass fiber, Polyamide 66

1 Introduction

The use of short fibre reinforced thermoplastic composites is rapidly growing, because of their high specific properties. Their good mechanical and chemical properties, low weight and ease of processing in complex forms would make them a reliable substitute for metallic materials. Moreover, fibre composite materials are used in automotive applications, under the hood where environmental conditions are very severe.

Large number of mechanical components are subjected to cyclic loading in their real operating conditions, which may causes fatigue failure even for loading levels below the elastic limit of the material. Therefore, the knowledge of the fatigue behaviour and mechanical properties of composite materials is vital, to optimize the design, to ensure the reliability and to guarantee the safe service use of components made of these materials. However, short glass fibre reinforced polyamide (PA-GFs) are very inhomogeneous since their mechanical properties result from the combination of the matrix, the glass fibres and of the interface (matrix/glass fibre) properties. Consequently, the mechanical behaviour of PA-GFs is a quite complex phenomenon since it is influenced by a large number of loading and structural parameter. Their mechanical properties are governed by the diameter, the length, the orientation and the quantity of fibres [1, 2]. Also processing conditions: speed and pressure of injection and temperature of the mould may affect the behaviour of composite material [3]. Experimental variables (deformation speed, test temperature, frequency, etc.) have an important influence on the fatigue behaviour of these materials [4-7]. Environmental conditions such, as temperatures and humidity are very important consideration. In the open literature, the effect of several parameters on the fatigue behaviour of PA-GFs was studied.

Several early studies have dealt with the influence of ambient temperature on the fatigue behaviour of PA66-GFs. It was shown that ambient temperature effect is related to the glass transition temperature (T_g) of the studied material. Handa et al. [8], demonstrated that temperature has no significant effect on the slope and the intercept of the S-N curve in the high-temperature region (above T_g). However for temperature

¹ Mechanical Modeling and Manufacturing Laboratory (LA2MP),
National Engineering School of Sfax, University of Sfax,
B.P W3038, Sfax, Tunisia

* Corresponding author, e-mail: mondherwali@yahoo.fr

ranges below T_g , the slope and intercept of the approximated S-N curve, tended to decrease with increasing temperature. These results were confirmed by Noda et al. [9].

Moreover, Jia and Kagan [10] found that the highest fatigue strength was reached at -40°C , and fatigue strength significantly reduced at elevated temperatures. In the study of Sonsino and Moosbrugger [11] and de Monte et al. [12], the same results was found. Furthermore, they found that the slopes of the Wohler-curves remain nearly constant.

Cyclic frequency effect on the fatigue behaviour of PA66-GF was investigated. It was found that increasing the frequency induces a self-heating phenomenon resulting from viscoelastic nature of the matrix and frictional heating in the composite [8]. The higher the frequency is the smaller the fatigue life is [9, 11, 13]. In the study of Bellenger et al. [14], two fracture modes were established: (i) a thermal mode when the temperature of the material can increase without equilibrium plateau until the sample fracture occurs and (ii) a mechanical mode governed by crack initiation and propagation. They conclude that both thermal and mechanical fractures occur at 10 Hz frequency. At 2 Hz frequency, the fracture is only mechanical and the matrix is still in the glassy state at break. Moreover, Zhou and Mallick [15] concluded that at frequencies less than 2 Hz, the failure mode was due to fatigue and the fatigue life increased with frequency. However, at frequencies greater than 2 Hz, a combination of fatigue and thermal failures took place and the fatigue life decreased with increasing frequency.

A common technique to produce PA66-GFs is the injection moulding process. This technique affect the orientation of fibres, which induces material anisotropy. Influence of this parameter is investigate using test specimens machined in different locations and at different orientations with respect to the injection moulding flow direction. Bernasconi et al. [16] showed that increasing specimen orientation angle decreases elastic modulus, ultimate tensile stress and fatigue strength. The same results was found by Zhou and Mallick [15] and Brunbauer et al. [17]. Recently, Benaarbia et al. [18], reported that ratcheting for fibre reinforced composites oriented at 45° and 90° was much higher than that for 0° composites

Moreover, Mallick and Zhou [19] evaluated the effect of the stress ratio on the fatigue behaviour of the PA66-GF33. Results of this research emphasize reduction in fatigue strength with increasing tensile mean stress. Moreover, Sonsino and Moosbrugger [11] demonstrated that mean-stresses diminish the endurable stress amplitude.

Moreover Barbouchi et al. [20] investigated water absorption influences on the fatigue behaviour of PA66-GFs. They found that the endurance limit at 10^7 cycles is greater for dried samples than for the humid samples. In Rajeesh et al. [21], the modulus and tensile strength were found to be decreasing because of the plasticization effect due to water absorption. Furthermore, Bernasconi et al. [22] showed that stiffness, tensile strength and

fatigue strength for wet specimen are considerably lower than those of the dry as moulded material. In addition, the slope of S-N curves decreased with water absorption.

Arif et al. [23] proved that the damage of a PA66-GF30 composite was mainly developed in the interfacial bonding of the fibre and the matrix, despite the fact that, matrix micro-cracks were dominant at the core layer perpendicular to the flow direction.

Many other parameters can affect the fatigue behaviour of PA-GF. For a review of parameters affecting the fatigue behaviour of composites materials in general, the reader is referred to Wicaksono and Chai [24].

Loading condition, stress ratio, amplitude of the applied loading and frequency are indeed very important factors that affect the fatigue behaviour of PA66-GFs, moreover the fiber content leads to variation of the mechanical properties of these materials. In this framework, the present paper intends to investigate and model the fatigue behaviour of PA66-GF. The emphasis of this work is on the effect of loading amplitude and fibre content. Quasi-static and fatigue tests were conducted for two different fibre percentages. S-N curves and curves for the force acting in the composite specimen are deduced. Based on the variation of elasticity modulus a new fatigue damage model is presented to predict the damage growth. The proposed model was used to predict damage evolution results, which was then compared with experimental results. A good agreement between experimental and numerical results is observed.

2 Material and experimental techniques

The material investigated in this study is a short glass fiber reinforced polyamide-66 containing 30% wt and 20%wt of short glass fibres. These materials are obtained by combination of two commercial products produced by Radici Plastics (RADICI GROUP) and commercially available under the trade name of Heramid A NAT (PA66) and A NAT FV030 (PA66-GF30). Specimens for tensile tests are types 1A, according to ISO 527-2 standard. However, fatigue test specimens were milled from moulded plates. Therefore ISO 527-2 specimens and rectangular plates, $125\pm 0.5 \times 105\pm 0.5 \times 4\pm 0.1$ mm, were injection moulded as shown in Fig. 1.

Specimens for fatigue testing were cut in the flow direction to dimensions of 115 ± 0.5 mm long by 15 ± 0.1 mm wide, 4 ± 0.1 mm thicknesses on a water-cooled CNC machine with a diamond coated carbide end mill. They were named PA66-GFxx as shown in Fig. 2. (Here the xx stands for the fiber content)

The elastic properties of the studied composite were measured according to ISO 527-1 standard. The tensile tests were carried out with a 10 kN Instron machine equipped with a RUDLPH laser extensometer under cross head speed of 1 mm/min as specified in ISO 527-1 standard.

Investigations of fatigue behavior of composite materials have been done using various fatigue experiments.

Uniaxial tension or compression fatigue tests were preferred. However, many researchers used bending fatigue experiments [13, 14, 21, 25-29] among others. In this paper, displacement-controlled bending fatigue tests have been used to provide the experimental results. This type of experiment was preferred because the geometry and loading conditions are very simple. Moreover, stresses and strains can vary along the gage length of the specimen. Furthermore, in bending tests, a different behavior and damage development of the specimen at the tension and compression side can be monitored. In addition, stress redistribution through the specimen thickness can be observed. Fatigue tests were performed using the in-house developed flexural fatigue experimental device as shown in Fig. 3.

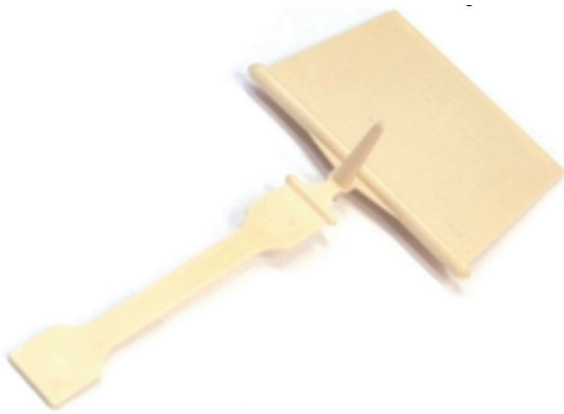


Fig. 1 Molded plates and ISO 527 specimens

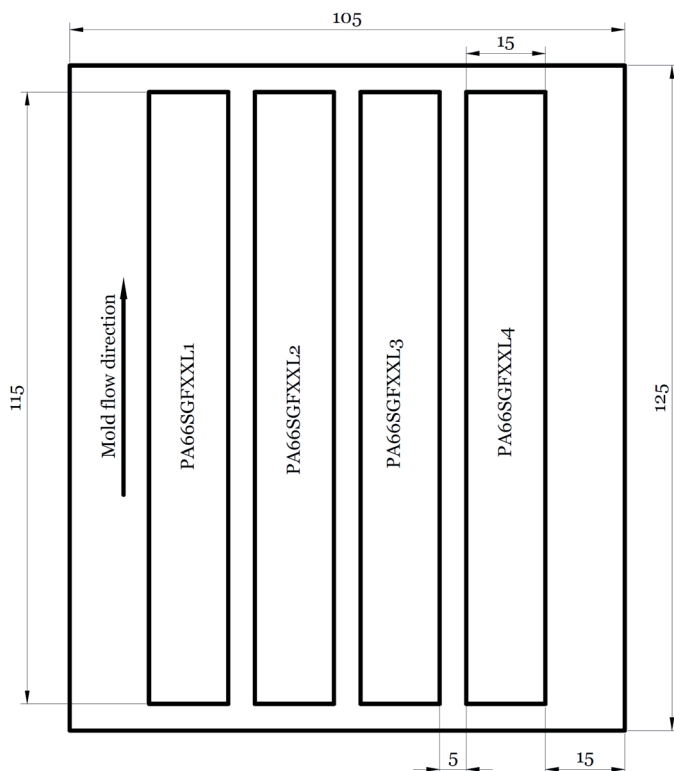


Fig. 2 Specimen dimensions milled from injection molded plates (dimensions are in mm)

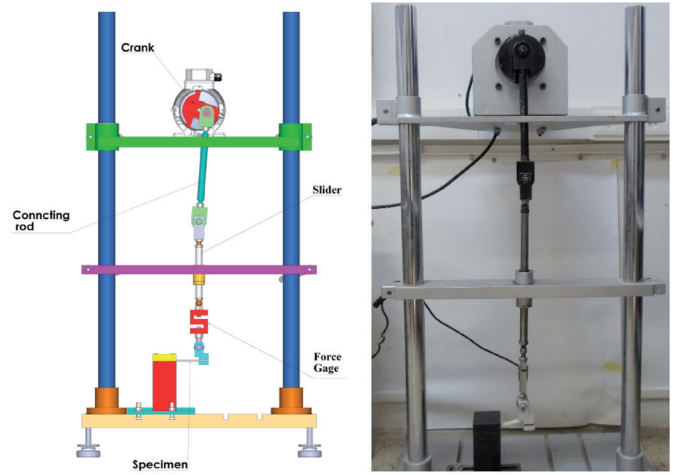


Fig. 3 Experimental fatigue setup

The outcoming shaft of the motor has a rotational speed of 1500 rpm. A variable-frequency drive is used to provide different fatigue testing frequencies. The alternating displacement ($u(t)$) is imposed using an adjustable crank-linkage mechanism. This mechanism imposes an alternating movement to the slider through the connecting rod. At the end of the slider, a force gage is connected to the specimen fixture in order to measure the force acting in the composite specimen. The other end of the specimen is clamped using four clamping bolts at equal constant torque. Hence, the specimen is loaded as clamped-clamped beam with one moving clamp (Fig. 4). The amplitude of the imposed displacement can be varied using the adjustable crank. The displacement ratio ($R_d = u_{\min} / u_{\max}$), analogue to the load ratio, can be chosen by adjusting a nut screw system.

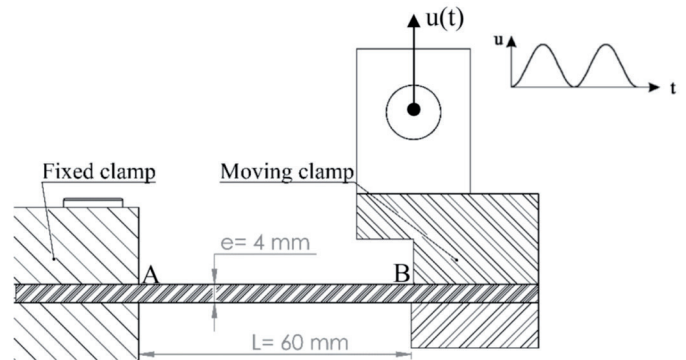


Fig. 4 Specimen fixture and boundary conditions

All the fatigue tests were carried out at room temperature under constant sinusoidal displacement with a displacement ratio $R_u = 0$ at 23°C. Load cycles were applied with a cyclic frequency of 2 Hz, in order to reduce the temperature increase of the specimen due to the self-heating phenomena Handa et al. [8]. The force acting on the specimen and displacement data were continuously recorded. Various experiments were performed in which the maximum applied displacement (u_{\max}) varied between 8 mm and 12.5 mm. At least three tests were performed for every applied displacement.

Figure 5 illustrates the beam model and the real deformed specimen. The specimen is considered as a clamped-clamped beam, with a fixed end and (Point A) a moving end (Point B). At the moving clamp, an alternating displacement $u_B = u_{Max}$ is imposed. The bending length is 60 mm. Figure 5b shows the real deformed configuration which justify the analytical assumptions.

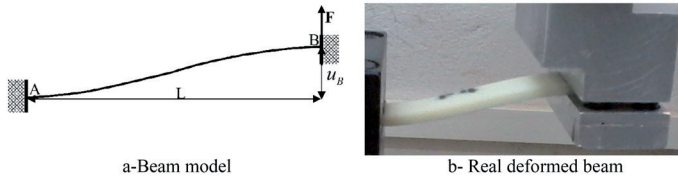


Fig. 5 Analytical model and real deformed beam

The corresponding force F , necessary to impose the bending displacement, is given by the following equation.

$$F = \frac{Ebh^3}{L^3}u_B \quad (1)$$

Where h is the specimen thickness, b is the specimen width and L is the bending length.

According to the bending moment distribution, the most constraint part correspond to the point A, the maximum induced stress in that particular point is given by the following equation

$$\sigma_{Max} = \frac{3FL}{bh^2} \quad (2)$$

A finite element simulation is performed to validate the proposed analytical model. The specimen is clamped in one end and in the other end a surface is constraint to a rigid body. An imposed displacement is applied to the rigid body (Fig. 6). Analytical, finite element and experimental results are compared as shown in Fig. 7. and Fig. 8. It is worthwhile to note the good agreement between the found results.

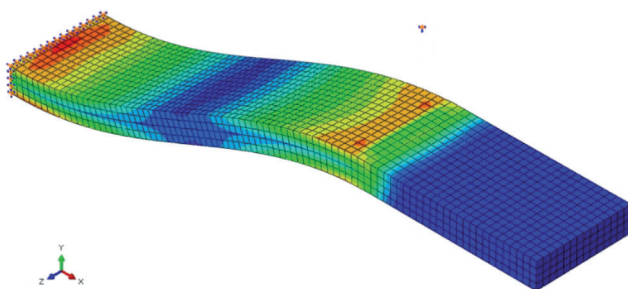


Fig. 6 Finite element model

3 Experimental results

3.1 Quasi-static results

Stress-strain curves of the studied composites under tensile tests are shown in Fig. 9. The higher fiber content is the higher the mechanical properties. Increasing the fiber content leads to an increase in tensile strength (σ_R) and elastic modulus. However,

the deformation capabilities are reduced. A loss of ductility is observed, PA66GFs present brittle behavior with small failure strain (ε_R), whereas the unfilled polyamide presents ductile behavior with large failure strain (Table 1). These results are in good agreement with those published by Ghorbel et al. [6].

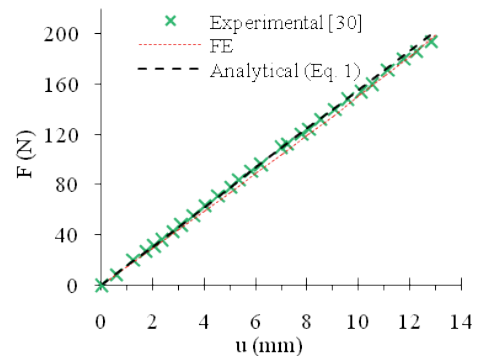


Fig. 7 Bending test. Load-displacement curves for PA66-GF30

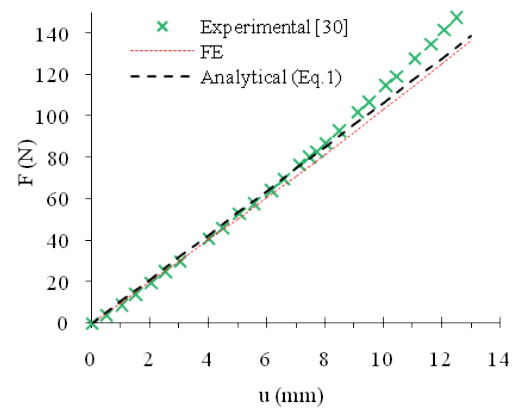


Fig. 8 Bending test. Load-displacement curves for PA66-GF20

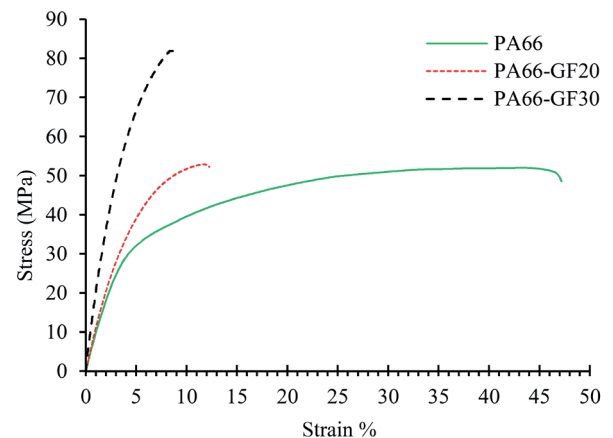


Fig. 9 Stress-strain curves under tensile tests

Table 1 Mechanical characteristics of the studied materials

| | PA66 | PA66-GF20 | PA66-GF30 |
|---------------------|------|-----------|-----------|
| E(MPa) | 1125 | 1927 | 3341 |
| σ_R (MPa) | 48 | 52.02 | 73.6 |
| ε_R (%) | 42.6 | 13.6 | 9.15 |

3.2 Fatigue results

Material stiffness degradation is used as a measure of damage accumulation in order to monitor and understand the damaging mechanism of fatigue loaded composite material throughout the service life. Although bending fatigue tests are not commonly used in fatigue investigation, they are preferred by many researchers [25-29]. The use of these tests is justified by the facts that: (i) Mechanical components are often loaded in bending in service conditions. (ii) The buckling effect is avoided when compared to tension/compression fatigue. (iii) Stresses, strains and damage distribution vary along the gauge length of the specimen, which allows studying fatigue damage in more complicated conditions. (iv) The required forces for bending fatigue are much smaller than those required for tension/compression fatigue tests.

To evaluate the stiffness degradation and damage growth in the studied material fatigue experiments were performed with different values of the imposed displacement. The complete time history of the stiffness degradation recorded is shown in Fig. 10. The maximum force acting in the composite specimen is deduced from these results. It is worthwhile to note the three stage of stiffness degradation defined by Van Paepegem and Degrieck [29], Nouri et al. [31] and Bellenger et al. [13] among others.

The specimen behavior exhibits three distinct stages of stiffness degradation during displacement controlled bending fatigue tests: (i) The first stage shows rapid stiffness reduction caused by the development of matrix micro-voids; (ii) In the second stage, the dominant damage mechanisms are coalescence and propagation of the micro-cracks. A gradual stiffness reduction of the material occurs in an approximately linear manner. The majority of fatigue life is categorized under this region. (iii) The last stage is characterized by sudden stiffness reduction followed by total failure. The most dominant failure in this region is fiber fracture and macroscopic crack propagation [14, 31].

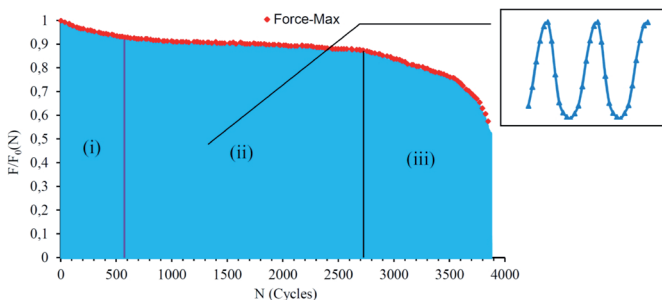
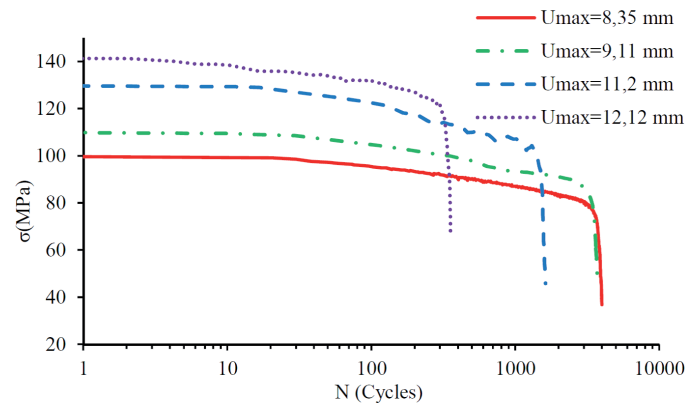


Fig. 10 Finite element model

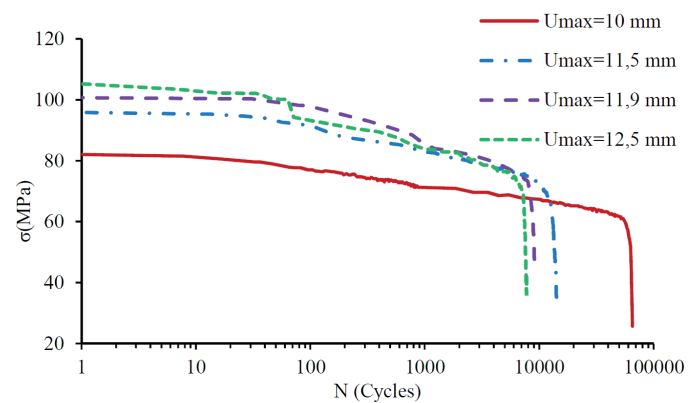
The evolution of the maximum induced stress acting in the composite specimen versus the number of cycles is shown in Fig. 11 and 12 using logarithmic scale. The higher applied displacement is the higher the initial force acting in the composite specimen. The curves display three stages: The first stage is characterized by a decrease of the material rigidity

corresponding to the material accommodation phase. In the first few cycles, the loss of material stiffness is rapid (Fig. 11 and Fig. 12). In the second stage, the force acting in the composite specimen decreases rapidly due to fiber breakage. The last stage corresponds to crack propagation and coalescence until sudden rupture. Furthermore, increasing applied displacement amplitude reduces the fatigue life without modifying the damage kinetic. Increasing fiber percentage increases the rigidity of the composite material. Therefore, for the same applied displacement the specimen with the higher fiber content has the lowest fatigue life.



(b) Logarithmic scale

Fig. 11 Evolution of the induced stress versus the number of cycles (PA66-GF30)



(c) Logarithmic scale

Fig. 12 Evolution of the induced stress versus the number of cycles (PA66-GF20)

Figure 13 shows typical failure mode of a PA66-GF20 specimen subjected to fatigue loading under a prescribed displacement of 8.85 mm. The clumped section was broken within the tension side. However, no observable damage was detected in the moving section. Failure started from tensile loaded side to compressive loaded side of the specimen.



Fig. 13 Typical failure mode (PA66-GF20)

The fatigue behavior of the studied materials is investigated through the S–N curves. The maximum initial applied stress versus the number of cycles to failure is reported in Fig. 14. The points related to the different fatigue tests fall into a line, which can be fitted according to Noda et al. [9] by the following equation

$$\sigma_{\max} = -A \log N + B \quad (3)$$

Where A is the slope of the S–N curve, which means the sensitivity of the fatigue resistance and B, is the intercept donating the apparent flexural strength. The values of these fatigue constants are listed in Table 2.

Table 2 Values of A and B for the two studied composites

| | A(MPa) | B(MPa) |
|-----------|--------|--------|
| PA66-GF20 | 10.2 | 196 |
| PA66-GF30 | 26.07 | 320.82 |

The S–N curves shown in Fig. 14 display the same shape, hence the same kinetic of fatigue. However, curves have different slopes and intercepts. Hence, the fiber content has a significant effect on the sensitivity of the fatigue resistance (A) and on the apparent flexural strength (B). Moreover, for nearly the same initial applied maximal stress, the higher the fiber content is the lower the fatigue life is. Therefore, we can conclude that increasing the fiber content leads to more fragile structure, which reduces the fatigue life under fatigue bending condition.

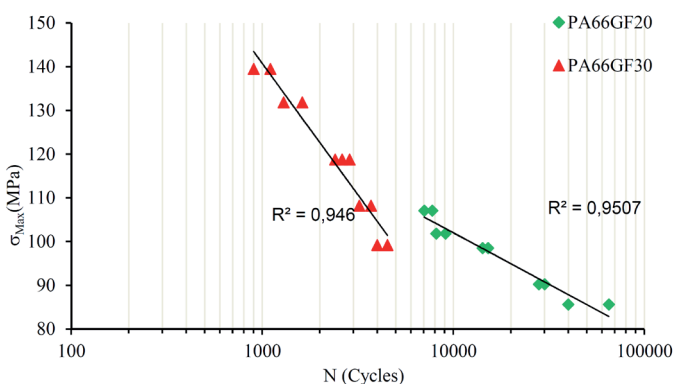


Fig. 14 Finite element model

4 Fatigue damage model

In the present study, a unidirectional model for fatigue damage is proposed. One local damage variable D is associated with the longitudinal stiffness loss. Hence, the fatigue damage law applies to uniaxial loading conditions. The stresses and strains are related by the following equation

$$\sigma = (1 - D) E_0 \varepsilon \quad (4)$$

where E_0 is the initial modulus.

The damage development of composite materials can be described by stiffness degradation of materials under fatigue loading. The elastic modulus reduction can be used as damage tracer. The experimental results show that the measured Young's modulus or stiffness just before complete failure of the specimen is not zero, thus, the damage variable is defined as [32]

$$D = \frac{E_0 - E}{E_0 - E_f} \quad (5)$$

where E is the residual Young's modulus and E_f is the Young's modulus toward the end of life. The residual modulus is calculated using the following equation

$$E = \frac{FL^3}{bh^3 u_B} \quad (6)$$

A fatigue damage model, very similar to the model proposed by Chaboche [33] and Wu and Yao [34] is presented to describe the stiffness degradation rule of composite materials in the loading direction. The proposed fatigue damage model can be specified as

$$D = 1 - \left(1 - \left(\frac{N}{N_f} \right)^\alpha \right)^\beta \quad (7)$$

N_f is the fatigue cycle number until failure, N is the current number of cycle, α and β are model parameters and D is the fatigue damage parameter.

Based on the experimental results, least square fitting procedure using the modified algorithm of Levenberg Marquardt was applied to determine the Model parameters. The function that defines the least-squares problem can be written as

$$F = \min \sum_{test=1}^{nt} \sum_{pt=1}^{np} \left(1 - \frac{D_{Exp}}{D_{Num}} \right)^2 \quad (8)$$

nt is the number of test for each material, np is the number of experimental points for each test, D_{Exp} is the damage experimental value (Eq. (5)) and D_{Num} is the damage numerical value (Eq. (7)).

The obtained values of the model parameters are listed out in Table 3.

Table 3 Values of the parameters of the presented model

| | α | β |
|-----------|----------|---------|
| PA66-GF20 | 0.117 | 0.202 |
| PA66-GF30 | 0.206 | 0.154 |

Curves presented in Fig. 15, to Fig. 20 give the fatigue damage growth obtained under different loading amplitude for two different fiber contents.

Fatigue damage curves shows three stages: In the first stage, multiple damage modes are acting within the material and the fatigue damage raises rapidly. The damage increases in a linear manner during the second stage due to crack growth and coalescence until it reaches saturation. In the final stage fiber failure, interfacial debonding leads to the sudden failure of the composite material. These results are in good agreement with experimental observation found by Reifsnider [35]. It is worthwhile to note that there is a good agreement between experimental results and numerical ones.

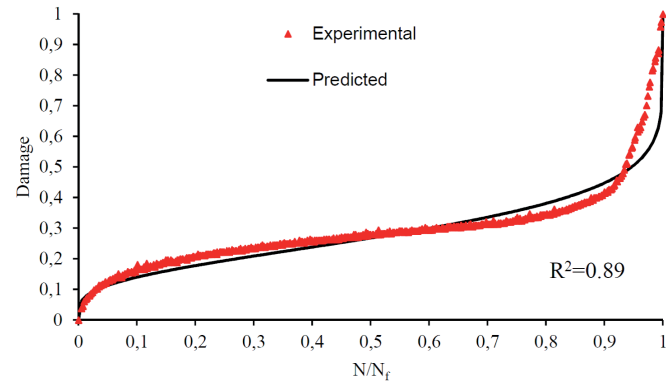


Fig. 15 Damage growth under imposed displacement
 $u_{\max} = 8.35$ mm (PA66-GF30)

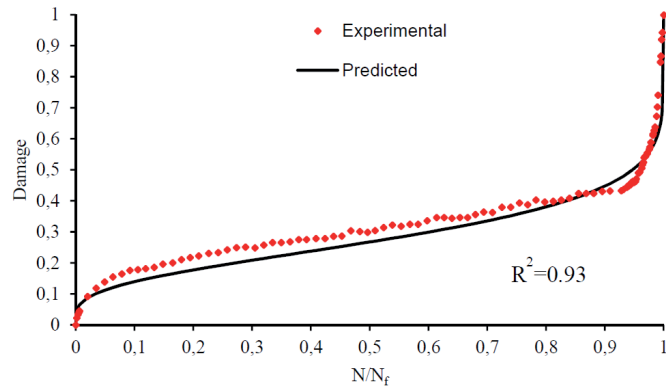


Fig. 16 Damage growth under imposed displacement
 $u_{\max} = 9.11$ mm (PA66-GF30)

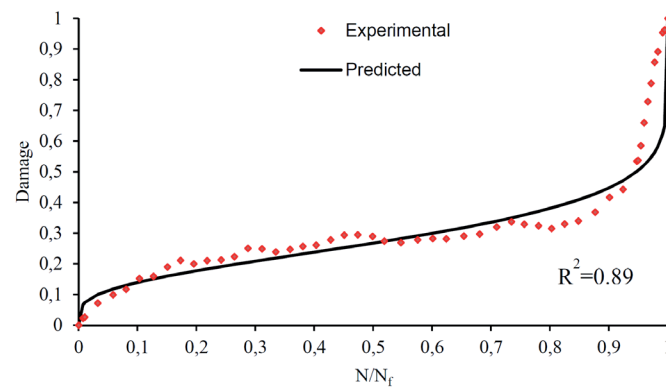


Fig. 17 Damage growth under imposed displacement
 $u_{\max} = 11.2$ mm (PA66-GF30)

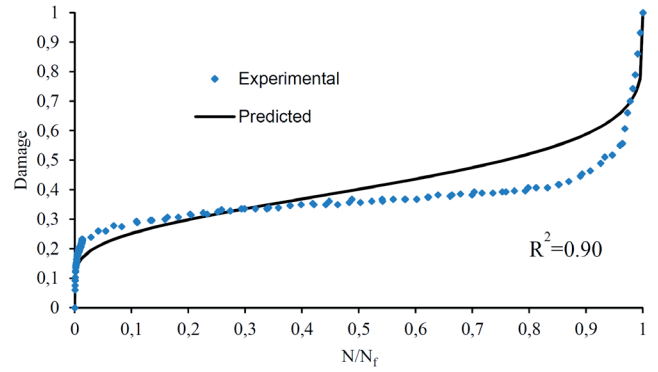


Fig. 18 Damage growth under imposed displacement
 $u_{\max} = 10$ mm (PA66-GF20)

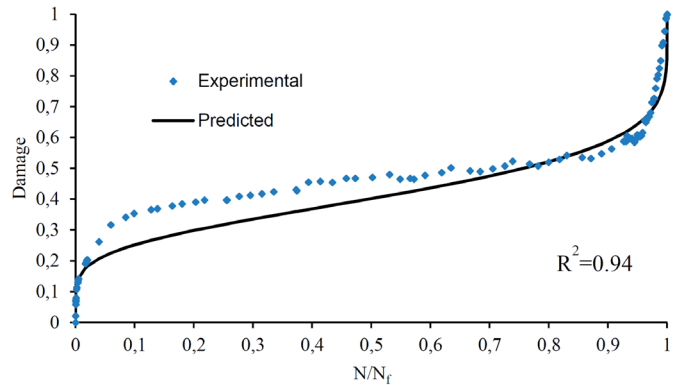


Fig. 19 Damage growth under imposed displacement
 $u_{\max} = 11.5$ mm (PA66-GF20)

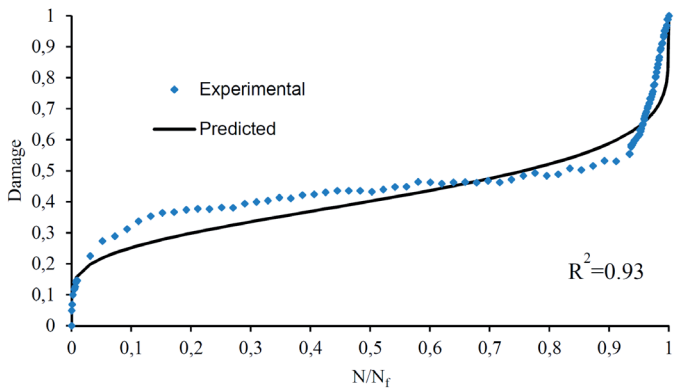


Fig. 20 Damage growth under imposed displacement
 $u_{\max} = 12.5$ mm (PA66-GF20)

5 Conclusion

This paper has discussed several topics concerning fatigue damage of short glass reinforced polyamide. The quasi-static elastic properties of the composite material are enhanced, increase in the elastic modulus and tensile strength, with increasing glass fiber content. However, the rupture behavior changes from ductile to brittle. The effect of fiber percentage on the fatigue behavior of short glass fiber reinforced polyamide is investigated. Damage growth kinetic is not affected by the fiber content. However increasing the fiber content decreases the fatigue life. Based on the stiffness degradation of composite

materials under fatigue loading, a phenomenological fatigue damage model is presented. Comparison between analytical and experimental results shows the ability of the proposed model to describe damage evolution in composite materials. The developed model herein describes with acceptable accuracy the three stages of damage growth found experimentally.

References

- [1] Thomason, J. L. "The influence of fibre properties of the performance of glass-fibre-reinforced polyamide 6,6." *Composites Science and Technology*. 59(16), pp. 2315-2328. 1999. DOI: [10.1016/S0266-3538\(99\)00083-4](https://doi.org/10.1016/S0266-3538(99)00083-4)
- [2] O'Regan, D. F., Akay, M., Meenan, B. "A comparison of Young's modulus predictions in fibre-reinforced-polyamide injection mouldings." *Composites Science and Technology*. 59(3), pp. 419-427. 1999. DOI: [10.1016/S0266-3538\(98\)00089-X](https://doi.org/10.1016/S0266-3538(98)00089-X)
- [3] Güllü, A., Özdemir, A., Özdemir, E. "Experimental investigation of the effect of glass fibres on the mechanical properties of polypropylene (PP) and polyamide 6 (PA6) plastics." *Materials & Design*. 27(4), pp. 316-323. 2006. DOI: [10.1016/j.matdes.2004.10.013](https://doi.org/10.1016/j.matdes.2004.10.013)
- [4] Mouhmid, B., Imad, A., Benseddiq, N., Benmedakhène, S., Maazouz, A. "A study of the mechanical behaviour of a glass fibre reinforced polyamide 6,6: Experimental investigation." *Polymer Testing*. 25(4), pp. 544-552. 2006. DOI: [10.1016/j.polymertesting.2006.03.008](https://doi.org/10.1016/j.polymertesting.2006.03.008)
- [5] Benaceur, I., Othman, R., Guegan, P., Dhieb, A., Damek, F. "Sensitivity of the flow stress of nylon 6 and nylon 66 to strain-rate." *International Journal of Modern Physics B*. 2(9-11), pp. 1249-1254. 2008. DOI: [10.1142/S021797920804661X](https://doi.org/10.1142/S021797920804661X)
- [6] Ghorbel, A., Saintier, N., Dhiab, A., Dammak, F. "Étude du comportement mécanique d'un polyamide 66 chargé de fibres de verre courtes." (Mechanical behavior study of short glass fibre-reinforced polyamide 66.) *Mécanique & Industries*. 12(5), pp. 333-342. 2011. (in French) DOI: [10.1051/meca/2011104](https://doi.org/10.1051/meca/2011104)
- [7] Ramazani, S., Morshed, M., Ghane, M. "Effect of service temperature on structure and mechanical properties of polyamide 6 & 66 tyre cords." *Journal of Polymer Resarches*. 18(4), pp. 781-792. 2011. DOI: [10.1007/s10965-010-9475-4](https://doi.org/10.1007/s10965-010-9475-4)
- [8] Handa, K., Kato, A., Narisawa, I. "Fatigue characteristics of a glass-fiber-reinforced polyamide." *Journal of Applied Polymer Science*. 72(13), pp. 1783-1793. 1999. DOI: [10.1002/\(SICI\)1097-4628\(19990624\)72:13<1783::AID-APP14>3.0.CO;2-B](https://doi.org/10.1002/(SICI)1097-4628(19990624)72:13<1783::AID-APP14>3.0.CO;2-B)
- [9] Noda, K., Takahara, A., Kajiyama, T. "Fatigue failure mechanisms of short glass fiber reinforced nylon 66 based on nonlinear dynamic viscoelastic measurement." *Polymer*. 42(13), pp. 5803-5811. 2001. DOI: [10.1016/S0032-3861\(00\)00897-1](https://doi.org/10.1016/S0032-3861(00)00897-1)
- [10] Jia, N., Kagan, V. A. "Effects of time and temperature on the tension-tension fatigue behavior of short fiber reinforced polyamides." *Polymer Composites*. 19(4), pp. 408-414. 1998. DOI: [10.1002/pc.10114](https://doi.org/10.1002/pc.10114)
- [11] Sonsino, C. M., Moosbrugger, E. "Fatigue design of highly loaded short-glass-fibre reinforced polyamide parts in engine compartments." *International Journal of Fatigue*. 30(7), pp. 1279-1288. 2008. DOI: [10.1016/j.ijfatigue.2007.08.017](https://doi.org/10.1016/j.ijfatigue.2007.08.017)
- [12] De Monte, M., Moosbrugger, E., Quaresimin, M. "Influence of temperature and thickness on the off-axis behaviour of short glass fibre reinforced polyamide 6,6 – cyclic loading." *Composite Part A: Applied Science and Manufacturing*. 41(10), pp. 1368-1379. 2010. DOI: [10.1016/j.compositesa.2010.02.004](https://doi.org/10.1016/j.compositesa.2010.02.004)
- [13] Esmaellou, B., Ferreira, P., Bellenger, V., Tcharkhtchi, A. "Fatigue behavior of polyamide 66/glass fiber under various kinds of applied load." *Polymer Composites*. 33(4), pp. 540-547. 2012. DOI: [10.1002/pc.22185](https://doi.org/10.1002/pc.22185)
- [14] Bellenger, V., Tcharkhtchi, A., Castaing, Ph. "Thermal and mechanical fatigue of a PA66/glass fibers composite material." *International Journal of Fatigue*. 28(10), pp. 1348-1352. 2006. DOI: [10.1016/j.ijfatigue.2006.02.031](https://doi.org/10.1016/j.ijfatigue.2006.02.031)
- [15] Zhou, Y. X., Mallick, P. K. "Fatigue performance of an injection-molded short E-glass fiber-reinforced polyamide 6,6. I. Effects of orientation, holes, and weld line." *Polymer Composites*. 27(2), pp. 230-237. 2006. DOI: [10.1002/pc.20182](https://doi.org/10.1002/pc.20182)
- [16] Bernasconi, A., Davoli P., Basile A., Filippi A. "Effect of fibre orientation on the fatigue behaviour of a short glass fibre reinforced polyamide-6." *International Journal of Fatigue*. 29(2), pp.199-208. 2007. DOI: [10.1016/j.ijfatigue.2006.04.001](https://doi.org/10.1016/j.ijfatigue.2006.04.001)
- [17] Brunbauer, J., Mösenbacher, A., Guster, C., Pinter, G. "Fundamental influences on quasistatic and cyclic material behavior of short glass fiber reinforced polyamide illustrated on microscopic scale." *Journal of Applied Polymer Science*. 131(19), Article number: 40842. 2014. DOI: [10.1002/app.40842](https://doi.org/10.1002/app.40842)
- [18] Benaarbia, A., Chrysochoos, A., Robert, G. "Thermomechanical behavior of PA6.6 composites subjected to low cycle fatigue." *Composites Part B: Engineering*. 76, pp. 52-64. 2015. DOI: [10.1016/j.compositesb.2015.02.011](https://doi.org/10.1016/j.compositesb.2015.02.011)
- [19] Mallick, P. K., Zhou, Y. "Effect of mean stress on the stress-controlled fatigue of a short E-glass fiber reinforced polyamide-6,6." *International Journal of Fatigue*. 26(9), pp. 941-946. 2004. DOI: [10.1016/j.ijfatigue.2004.02.003](https://doi.org/10.1016/j.ijfatigue.2004.02.003)
- [20] Barbouchi, S., Bellenger, V., Tcharkhtchi, A., Castaing, P., Jollivet, T. "Effect of water on the fatigue behaviour of a pa66/glass fibers composite material." *Journal of Materials Science*. 42(6), pp. 2181-2188. 2007. DOI: [10.1007/s10853-006-1011-x](https://doi.org/10.1007/s10853-006-1011-x)
- [21] Rajeeesh, K. R., Gnanamoorthy, R. Velmurugan, R. "The effect of moisture content on the tensile behaviour of polyamide 6 nanocomposites." *Proceedings of the Institution of Mechanical Engineers, Part L: Journal of Materials: Design and Applications*. 224(4), pp. 173-176. 2010. DOI: [10.1243/14644207JMDA316](https://doi.org/10.1243/14644207JMDA316)
- [22] Bernasconi, A., Davoli, P., Rossin, D., Armani, C. "Effect of reprocessing on the fatigue strength of a fiber glass reinforced polyamide." *Composites Part A: Applied Science and Manufacturing*. 38(3), pp. 710-718. 2007. DOI: [10.1016/j.compositesa.2006.09.012](https://doi.org/10.1016/j.compositesa.2006.09.012)
- [23] Arif, M. F., Saintier, N., Meraghni, F., Fitoussi, J., Chemisky, Y., Robert, G. M. "Multiscale fatigue damage characterization in short glass fiber reinforced polyamide-66." *Composites Part B: Engineering*. 61, pp. 55-65. 2014. DOI: [10.1016/j.compositesb.2014.01.019](https://doi.org/10.1016/j.compositesb.2014.01.019)
- [24] Wicaksono, S., Chai, GB. "A review of advances in fatigue and life prediction of fiber-reinforced composites." *Proceedings of the Institution of Mechanical Engineers, Part L: Journal of Materials: Design and Applications*. 227(3), pp. 179-195. 2013. DOI: [10.1177/1464420712458201](https://doi.org/10.1177/1464420712458201)
- [25] Sidoroff, F., Subagio B. "Fatigue damage modelling of composite materials from bending tests." In: Matthews, F. L., Buskell, N. C. R., Hodgkinson, J. M., Morton, J. (eds.) Sixth international conference on composite materials (ICCM-VI) & Second European Conference on Composite Materials (ECCM-II): proceedings, Vol. 4., London, UK, Jul. 20-24, 1987. Elsevier; 1987, pp. 4.32-4.39.
- [26] Caprino, G., D'Amore, A. "Flexural fatigue behaviour of random continuous-fibre reinforced thermoplastic composites." *Composites Science and Technology*. 58(6), pp. 957-965. 1998. DOI: [10.1016/S0266-3538\(97\)00221-2](https://doi.org/10.1016/S0266-3538(97)00221-2)

- [27] De Baere, I., Van Paepegem, W., Degrieck, J. "Comparison of different setups for fatigue testing of thin composite laminates in bending." *International Journal of Fatigue*. 31(6), pp. 1095-1101. 2009. DOI: [10.1016/j.ijfatigue.2008.05.011](https://doi.org/10.1016/j.ijfatigue.2008.05.011)
- [28] Belingardi, G., Cavatorta, M. P. "Bending fatigue stiffness and strength degradation in carbon-glass/epoxy hybrid laminates: Cross-ply vs. angle-ply specimens." *International Journal of Fatigue*. 28(8), pp. 815-825. 2006. DOI: [10.1016/j.ijfatigue.2005.11.009](https://doi.org/10.1016/j.ijfatigue.2005.11.009)
- [29] Van Paepegem, W., Degrieck, J. "A new coupled approach of residual stiffness and strength for fatigue of fibre-reinforced composites." *International Journal of Fatigue*. 24(7), pp. 747-762. 2002. DOI: [10.1016/S0142-1123\(01\)00194-3](https://doi.org/10.1016/S0142-1123(01)00194-3)
- [30] Chebbi, E., Wali, M., Dammak, F. "An anisotropic hyperelastic constitutive model for short glass fiber-reinforced polyamide." *International Journal of Engineering Science*. 106, pp.262-272. 2016. DOI: [10.1016/j.ijengsci.2016.07.003](https://doi.org/10.1016/j.ijengsci.2016.07.003)
- [31] Nouri, H., Meraghni, F., Lory, P. "Fatigue damage model for injection-molded short glass fibre reinforced thermoplastics." *International Journal of Fatigue*. 31(5), pp. 934-942. 2009. DOI: [10.1016/j.ijfatigue.2008.10.002](https://doi.org/10.1016/j.ijfatigue.2008.10.002)
- [32] Mao, H., Mahadevan, S. "Fatigue damage modelling of composite materials." *Composite Structures*. 58(4), pp. 405-410. 2002. DOI: [10.1016/S0263-8223\(02\)00126-5](https://doi.org/10.1016/S0263-8223(02)00126-5)
- [33] Chaboche, J. L. "Une loi différentielle d'endommagement de fatigue avec cumulation non linéaire." (Differential Fatigue Damage Law with Nonlinear Cumulation.) *Revue Française de Mécanique*. 50-51, 1974. (in French)
- [34] Wu, F., Yao, W. "A fatigue damage model of composite materials." *International Journal of Fatigue*. 32(1), pp. 134-138. 2010. DOI: [10.1016/j.ijfatigue.2009.02.027](https://doi.org/10.1016/j.ijfatigue.2009.02.027)
- [35] Reifsnider, K. L., Henneke, E. G., Stinchcomb W. W., Duke, J. C. "Damage mechanics and NDE of composite laminates." In: *Mechanics of composite materials*. (Hashin, Z., Herakovich, C. T. (Recent advances)). pp. 399-420, Pergamon Press, New York, 1983. DOI: [10.1016/B978-0-08-029384-4.50032-8](https://doi.org/10.1016/B978-0-08-029384-4.50032-8)